ACS chemical biology

Articles

pubs.acs.org/acschemicalbiology

Mechanism and *In Vitro* Pharmacology of TAK1 Inhibition by (5*Z*)-7-Oxozeaenol

Jiaquan Wu,*[,†] Francoise Powell,[‡] Nicholas A. Larsen,[†] Zhongwu Lai,[‡] Kate F. Byth,[‡] Jon Read,[§] Rong-Fang Gu,[⊥] Mark Roth,[‡] Dorin Toader,[‡] Jamal Carlos Saeh,[‡] and Huawei Chen*[,‡]

[†]Discovery Sciences, [‡]Oncology Innovative Medicine Unit, and [⊥]Infection Innovative Medicine Unit, AstraZeneca R&D Boston, Waltham, Massachusetts 02451, United States

[§]Discovery Sciences, AstraZeneca R&D Alderley Park, Cheshire, England SK10 4TG

Supporting Information

ABSTRACT: Transforming growth factor-β activated kinase-1 (TAK1) is a member of the mitogen-activated protein kinase kinase kinase (MAP3K) family that regulates several signaling pathways including NF-κB signal transduction and p38 activation. TAK1 deregulation has been implicated in human diseases including cancer and inflammation. Here, we show that, in addition to its kinase activity, TAK1 has intrinsic ATPase activity, that (5*Z*)-7-Oxozeaenol irreversibly inhibits TAK1, and that sensitivity to (5*Z*)-7-Oxozeaenol inhibition in hematological cancer cell lines is NRAS mutation status and TAK1 pathway dependent. X-ray crystallographic and mass spectrometric studies showed that (5*Z*)-7-Oxozeaenol forms a covalent complex with TAK1. Detailed biochemical characterization revealed that (5*Z*)-7-Oxozeaenol inhibited both the kinase and the ATPase activity of TAK1 following a bi-phase kinetics, consistent with the irreversible inhibition mechanism. In DoHH2 cells, (5*Z*)-7-Oxozeaenol potently inhibited the p38 phosphorylation driven by TAK1, and the inhibition lasted over 6 h after withdrawal of (5*Z*)-7-Oxozeaenol. Profiling (5*Z*)-7-Oxozeaenol in a panel of hematological cancer cells showed that sensitive cell lines tended to carry NRAS mutations and that genes in TAK1 regulated pathways were enriched in sensitive cell lines. Taken together, we have elucidated the molecular mechanism of a TAK1 irreversible inhibitor and laid the foundation for designing next generation TAK1 irreversible inhibitors. The NRAS-TAK1-Wnt signaling network discerned in our study may prove to be useful in patient selection for TAK1 targeted agents in hematological cancers.

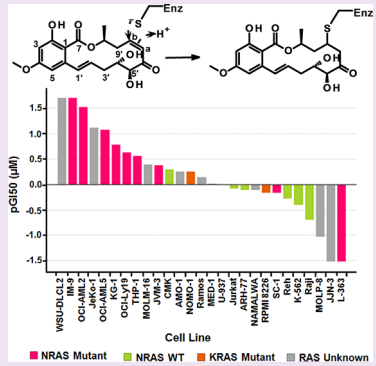

Over the past two decades, intensive research has been directed toward developing ATP competitive inhibitors for kinases. Great success has been achieved in obtaining inhibitors with picomolar affinity. However, it remains a key challenge to achieve kinase inhibitors with superior pharmacokinetic properties that can inhibit the target sufficiently. It is also difficult to obtain kinase inhibitors with desired selectivity profiles, due to the inherent similarity and high sequence conservation in the ATP binding pocket across the kinase family. Indeed, many kinase inhibitors display polypharmacology (inhibiting more than one target), and the biological significance of that is often not well understood.[1] The strategy of exploiting the less conserved interactions in the back-pocket of kinases, locking the activation loop in a DFG-out conformation, has worked well for a number of kinases. Even though the finding of DFG-out binding nature of Bcr-Abl kinase inhibitor Gleevec was serendipitous in nature, the molecular level learning has been applied to design newer generations of DFG-out binders. Induction of major conformational changes by this type of binding interaction is often kinase-inhibitor pair specific and can significantly alter the on- and off-rates to affect the inhibitor-target residence time for more desirable pharmacodynamic outcome.[1,2] Recently, irreversible kinase inhibitors have attracted attention as another strategy to improve selectivity and duration of inhibition.[3,4] Here we show that irreversible inhibition is a possible strategy for designing selective inhibitors against TAK1 kinase (transforming growth factor-β activated kinase-1, also known as MAP3K7 and MEKK7, EC 2.7.11.25).

TAK1 is a serine/threonine kinase and belongs to the mitogen-activated protein kinase kinase kinase (MAP3K) family that controls a variety of cell functions.[5-8] For example, TAK1 is an essential mediator of antigen receptor signaling in B and T lymphocytes and is involved in the interleukin-1 (IL-1) signaling pathway.[8-10] Stimulation of cells by IL-1 leads to the activation of TAK1, which stimulates the MAPK cascade and IKKs, leading to the activation of JNK/p38 MAPKs and NF-κB. TAK1 requires a protein activator, the TAK1-binding protein 1 (TAB1), to achieve its full activity.[11] It was later identified that the C-terminus of TAB1 plays an essential role in its binding to TAK1 and that residues from 437 to 504 amino acids of TAB1 are sufficient for full activation of TAK1 in HeLa cells.[12,13] The pivotal role that TAK1 plays in several often deregulated cellular pathways suggests it should be a potential target for

Received: October 30, 2012
Accepted: December 28, 2012
Published: December 28, 2012

Table 1. Kinetic Constants for TAK1 and (5*Z*)-7-Oxozeaenol

	TAK1-TAB1		TAK1/TAB1	(5*Z*)-7-Oxo/TAK1-TAB1	
	ATPase	kinase[a]	kinase[b]	irreversible binding	MS
K_M, ATP (μM)	9.0 ± 1.2	21 ± 1	24 ± 3		
k_{cat} (min^{-1})	6.0 ± 0.2	11.4			
k_3 (min^{-1})				0.23 ± 0.020	0.40 ± 0.040
k_4 (h^{-1})					
K_i^{app} (μM)				0.071 ± 0.032	
IC_{50} (μM)	0.014		0.009		

[a]Values are cited from ref 13. [b]Values were obtained using full-length TAK1/TAB1 with AlphaScreen assay using a kinase-dead mutant of biotin-MKK6 as substrate.

small molecule intervention to combat human diseases including cancer and inflammation. A class of resorcyclic acid lactones (RALs) including (5*Z*)-7-Oxozeaenol and hypothemycin has been reported to irreversibly inhibit MAPKs such as MEKs and ERK1/2.[14,15] In particular, (5*Z*)-7-Oxozeaenol, a natural product of fungal origin, was reported to be a TAK1 specific inhibitor.[16] In this report, taking advantage of the intrinsic ATPase activity of TAK1, we investigated the irreversible TAK1 inhibition mechanism of (5*Z*)-7-Oxozeaenol using multiple biochemical, biophysical, and biological methods. We also explored the pharmacological profile of (5*Z*)-7-Oxozeaenol in cancer cells and its relationship to TAK1 regulated genes and other important genetic markers.

RESULTS AND DISCUSSION

TAK1-TAB1 Protein Has Significant Intrinsic ATPase Activity. While investigating its kinase activity, we found that the TAK1-TAB1 fusion protein bears significant ATP hydrolysis activity in the absence of a protein or peptide substrate. We observed both TAK1-TAB1 protein concentration and time dependent ATP turnover using both the coupled PK/LDH assay and the Malachite Green assay. When the experiments were repeated with fully de-phosphorylated TAK1-TAB1, we observed a similar rate of ATP turnover. Mass spectrometry showed that de-phosphorylated TAK1-TAB1 (observed MW 35482 Da, expected MW 35478 Da) was di-phosphorylated (MW 35642 Da, +160 Da) upon incubation with ATP/Mg^{2+}, and the phosphorylation occurred spontaneously under these conditions. The high stoichiometry of ATP turnover to TAK1 enzyme concentration ruled out the possibility that the observed ATP consumption was driven by auto-phosphorylation of TAK1-TAB1. Furthermore, inorganic phosphate was produced (V_{max} = 2.3 ± 0.2 μM min^{-1}) at a similar rate as ADP generation (V_{max} =1.8 ± 0.2 μM min^{-1}). To confirm that the ATP hydrolysis activity is not an artifact resulting from the protein fusion rather from the intrinsic ATPase activity of TAK1 kinase, we repeated the same experiments using a protein complex of full length TAK1 and TAB1 (TAK1/TAB1), and results showed that the protein complex had specific ATP hydrolysis activity similar to that of the fusion protein. Further kinetic studies using coupled PK/LDH assay revealed that TAK1-TAB1 ATPase has an ATP K_M of 9.0 (±1.2) μM and a k_{cat} of 6.0 (±0.2) min^{-1}, both comparable to those determined in a TAK1-TAB1 kinase assay reported elsewhere[13] (Table 1). Additionally, this ATPase activity was inhibited by the TAK1 specific inhibitor (5*Z*)-7-Oxozeaenol with a potency similar to that for (5*Z*)-7-Oxozeaenol's inhibition of TAK1-TAB1 kinase activity (Table 1). Not surprisingly, similar to the observation with MEK kinase[17] and MAPKs,[18] the ATPase activity of TAK1-TAB1 was suppressed by a protein substrate. When the downstream substrate, a kinase-dead mutant of MKK6 protein, was present, we observed strong phosphorylation of the substrate by TAK1-TAB1 with no free phosphate formation.

Protein kinases with intrinsic ATPase activity are not uncommon. Several other protein kinases, especially kinases involved in MAPK pathways, have shown intrinsic ATPase activity.[15,17,18] The consequence of intrinsic ATPase activity of kinases under physiological conditions remains unknown. However, it appears that at least at the *in vitro* biochemical level, such activity is kinetically and structurally controlled. For most of the kinases with ATPase activity, the catalytic efficiency of ATPase activity is usually either equivalent to, or several fold to several orders lower than that of the phospho-transferase activity,[15,17,18] suggesting that in general the phosphorylation of downstream substrates is a more efficient event than the hydrolysis of ATP by these kinases. Furthermore, the inclusion of the downstream protein substrates was found to suppress the ATPase activity for all cases investigated so far, demonstrating that under physiological conditions the futile ATP hydrolysis by kinases might be prevented because all kinases are present in a form of complexes with cognate protein substrates or activators. Nonetheless, this intrinsic ATPase activity provided a convenient option for *in vitro* studies of kinases requiring full-length proteins as substrates. Taking advantage of the ATPase activity of TAK1 kinase we studied the mode of inhibition of TAK1 by (5*Z*)-7-Oxozeaenol and characterized it as an irreversible inhibitor of TAK1 kinase.

(5*Z*)-7-Oxozeaenol Inhibits TAK1-TAB1 Activity by Covalent Modification. (5*Z*)-7-Oxozeaenol was identified previously as a TAK1 specific inhibitor that blocked IL-1 induced NF-κB pathway activation in cells.[16] Importantly, this compound showed a time-dependent inhibition of TAK1 kinase activity, suggesting that (5*Z*)-7-Oxozeaenol is a slow onset inhibitor. It was suspected that (5*Z*)-7-Oxozeaenol inhibited TAK1 irreversibly in cells on the basis of the observation that TAK1 kinase activity was still inhibited 30 min after compound was removed from the cell culture. However, the delayed inhibitory effect could also be explained by reversible but slowly dissociating inhibition complex or simply (5*Z*)-7-Oxozeaenol being trapped inside cells. To fully elucidate the inhibition kinetics and covalent nature of the interaction, we set up to investigate the molecular mechanism of TAK1 inhibition by (5*Z*)-7-Oxozeaenol by means of mass spectrometry, pre-steady state kinetics, and X-ray crystallography.

Mass Spectrometry. (5*Z*)-7-Oxozeaenol contains a *cis*-enone at its 6′ to 8′ position that could function as a Michael acceptor for an appropriately positioned thiol functional group of cysteine residue of TAK1 to form an irreversible kinase–inhibitor complex. Protein mass spectrometry with stringent

dx.doi.org/10.1021/cb3005897 | *ACS Chem. Biol.* 2013, 8, 643–650

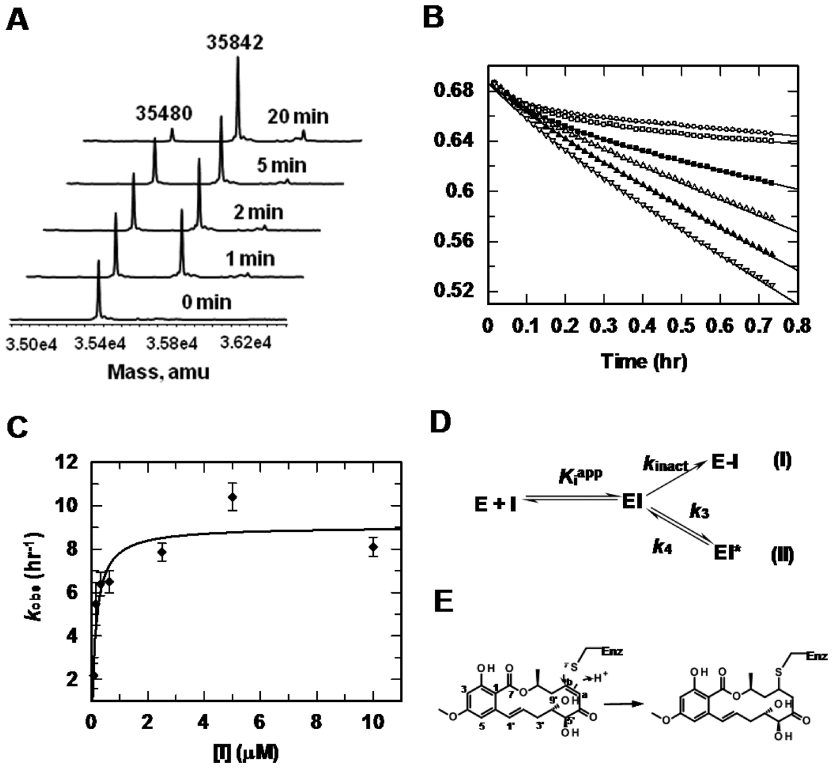

Figure 1. Biochemical characterization of (5*Z*)-7-Oxozeaenol inhibition. (A) MS traces of (5*Z*)-7-Oxozeaenol modification of TAK1-TAB1 protein. Experimental details are described in Methods. Molecular weight of each peak is labeled, with 35480 assigned to apo-TAK1-TAB1 and 35842 to (5*Z*)-7-Oxozeaenol-TAK1-TB1 adduct. (B) Progress curves for reactions of TAK1-TAB1 with ATP in the presence of varying concentrations of (5*Z*)-7-Oxozeaenol. Solid lines represent the best fit of each reaction by eq 1. ∇, DMSO; ▲, 0.078 μM (5*Z*)-7-Oxozeaenol; Δ, 0.156 μM (5*Z*)-7-Oxozeaenol; ■, 0.312 μM (5*Z*)-7-Oxozeaenol; □, 0.625 μM (5*Z*)-7-Oxozeaenol; ○, 5 μM (5*Z*)-7-Oxozeaenol. (C) Plot of apparent first-order rate constants (k_{obs}) of transition from v_i to v_s against (5*Z*)-7-Oxozeaenol concentrations. The solid line represents the best fit of the data to eq 2. (D) (5*Z*)-7-Oxozeaenol could modify TAK1-TAB1 *via* either covalent modification (I) or a slow on-set tight-binding mechanism (II). (E) The thiolate of Cys174 of TAK1-TAB1 undergoes nucleophilic attach on C8′ of the *cis*-enone of (5*Z*)-7-Oxozeaenol to form a covalent bond.

solubilizing conditions (0.1% formic acid and 5% methanol) gives a direct readout of whether there is any covalent modification of the protein and the stoichiometry of the interaction. Figure 1A shows time dependent modification of TAK1-TAB1 by (5*Z*)-7-Oxozeaenol. Experiments were carried out with both (5*Z*)-7-Oxozeaenol and TAK1-TAB1 protein at 1 μM. Under these conditions over 50% of TAK1-TAB1 (MW 35480 Da, predicted MW 35482 Da) was converted to a covalent protein−inhibitor complex (MW 35842 Da) within 1 min, and over 90% conversion was achieved within 20 min. The 362 Da molecular weight difference between the complex and the apo-protein indicated a mono-alkylation of TAK1-TAB1 protein by (5*Z*)-7-Oxozeaenol. The first-order rate constant of the initial phase of this modification was estimated to be 0.4 min^{-1} (Table 1).

Inhibition Kinetics. Having demonstrated by mass spectrometry that (5*Z*)-7-Oxozeaenol specifically alkylated TAK1-TAB1, we next investigated the kinetics of this event. In a coupled PK/LDH assay, progress curves for the reaction of TAK1-TAB1 with ATP in the presence of varying concentrations of (5*Z*)-7-Oxozeaenol showed that the reaction velocity decreased exponentially in a time-dependent manner, from an initial velocity v_i to a final, steady-state velocity v_s (Figure 1B). Higher concentrations of (5*Z*)-7-Oxozeaenol caused the steady-state to be reached more quickly with a reduced v_s. This behavior indicates that (5*Z*)-7-Oxozeaenol is either a slow, tight-binding reversible inhibitor, or an irreversible inhibitor that interacts rapidly with the enzyme to form an initial complex, EI, followed by a slow conversion to a covalent adduct, E-I (Figure 1D). Individual progress curves for the reaction of TAK1-TAB1 fit well to eq 1, which describes the irreversible inhibition mechanism, allowing values for v_i, v_s, and k_{obs} to be determined for each inhibitor concentration. Consistent with the mechanism shown in Figure 3D, k_{obs} displayed a hyperbolic dependence on (5*Z*)-7-Oxozeaenol concentration (Figure 1C), and nonlinear curve fitting using eq 2 gave values for k_{inact} and K_i^{app} (Table 1). A k_{inact} of 0.23 min^{-1} is very close to the observed rate of TAK1-TAB1 modification by MS (Table 1), further confirming the irreversible nature of (5*Z*)-7-Oxozeaenol inhibition on TAK1-TAB1.

X-ray Crystal Structure of (5Z)-7-Oxozeaenol Modified TAK1-TAB1. TAK1-TAB1 protein purified from insect cells is partially phosphorylated, as assessed by mass spectrometry. To obtain robust crystals, the purified TAK1-TAB1 protein was treated with λ-phosphatase to produce a homogeneous sample. TAK1-TAB1 crystals were then obtained by co-crystallization with adenosine, which is essential for growing quality crystals. Subsequently a series of back soaking experiments were performed with high concentration of (5*Z*)-7-Oxozeaenol to displace adenosine from the active site, resulting in a complex with (5*Z*)-7-Oxozeaenol at 2.2 Å resolution (Table 2).

TAK1 has the prototypic kinase domain with the N- and C-lobes linked together by the hinge. The interface between the two domains forms the kinase active site, where ATP binds. The majority of kinase inhibitors have a flat chemotype, mimicking the adenine ring of ATP. (5*Z*)-7-Oxozeanol is no

dx.doi.org/10.1021/cb3005897 | *ACS Chem. Biol.* 2013, 8, 643−650

Table 2. Crystallographic Data and Refinement

space group	*I*222
unit cell	$\alpha = \beta = \gamma = 90°$; a = 58.1, b = 133.9, c = 142.1 Å
mosaicity	1.26
wavelength	1.54 Å
resolution	2.2 Å
unique reflections	28551
multiplicity	6.0 (5.9)
completeness (%)	100.0 (100.0)
$I/\sigma(I)$	7.8 (2.0)
R_{merge}[a] (%)	0.094 (0.484)
R_{work}[b]/R_{free}[c] (%)	0.221/0.245
residues	326
waters	159
av *B* factor	
protein	64.8
inhibitor	67.9
water	64.1
Ramachandran	
most favored	90.4%
allowed	8.4%
generously allowed	1.2%
disallowed	0.0%

[a] $R_{merge} = \Sigma|I - \langle I\rangle|/\Sigma I$, where I is the integrated intensity of a given reflection and $\langle I\rangle$ is the average intensity of multiple observations of symmetry-related reflections. [b] $R_{work} = \Sigma|F_o - F_c|/\Sigma F_o)$, where F_o and F_c are observed and calculated structure factors. [c] R_{free} was calculated from a 5% subset of reflections that were excluded from the refinement. Parentheses indicate highest resolution shell.

exception, slotting between the N- and C-lobes that form the active site (Figure 2A). The electron density shows there is a covalent bond formed between the thiolate group of Cys174 and the C8′ of the *cis*-enone. Cys174 sits at the bottom of the pocket, immediately preceding the DFG sequence of the activation loop. These residues are in the DFG-in conformation. (5*Z*)-7-Oxozeaenol makes an H-bond to the hinge, between the benzylic hydroxyl at C2 and the backbone amide of Ala107 (Figure 2A). The benzylic methoxy group points toward the solvent channel, while the methyl at C10′ forms a VDW contact with the gatekeeper methionine residue. The macrolactone ring is sandwiched between Val50 from the N-lobe and Leu163 of the C-lobe. The 4′-OH of the macrolactone forms an H-bond with the backbone carbonyl of Pro160. The binding mode we observed is similar to that seen in the crystal structures of ERK2 bound to (5*Z*)-7-Oxozeaenol (FR148083),[14] and to hypothemycin.[19] The ERK2 structures also showed similar H-bonding interactions to the hinge and from the 4′-OH and backbone carbonyl.

The structure of TAK1 bound to adenosine superimposes closely on our structure bound to (5*Z*)-7-Oxozeaenol with an RMSD of 0.6 Å (Figure 2B). The differences between the two structures are minimal, with similar conformations in the DFG loop and the Gly-rich loop. The N- and C-lobes have the same relative orientation to each other. In order to bind ATP, there would have to be some conformational changes in the Gly-rich loop to provide enough room for the additional phosphate groups. Comparison of the two structures shows that the N1 atom of adenosine superimposes on the benzylic hydroxyl of (5*Z*)-7-Oxozeaenol (Figure 2B). The O3 hydroxyl of the ribose sugar does not form any interactions with the protein, but is in proximity to the 4′-OH of the macrolactone, suggesting the

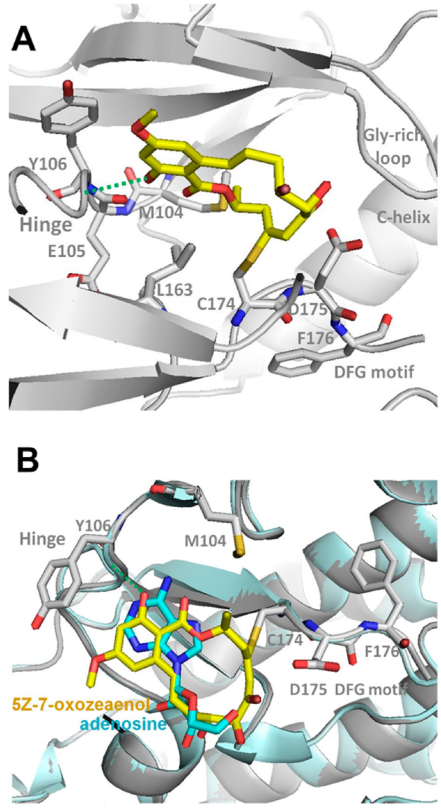

Figure 2. Structure of (5*Z*)-7-Oxozeaenol (yellow) bound to TAK1-TAB1 (gray). (A) The unsaturated *cis*-enone reacts with the thiolate of Cys174, forming a covalent, irreversible bond. The H-bond to the hinge is indicated by green dashed line. Residues Met, Glu, and Tyr from the hinge are shown, as well as Leu163 at the bottom of the pocket and the DFG motif. Met104 is the gatekeeper residue. (B) Superposition of the (5*Z*)-7-Oxozeaenol bound structure (gray) with the adenosine (cyan) bound structure (light blue). The structures superimpose very closely with minimal conformational changes. Adenosine and (5*Z*)-7-Oxozeaenol make one conserved H-bond interaction to the hinge (dashed green line).

potential for an interaction if the kinase conformation were to change.

(5Z)-7-Oxozeaenol Inhibits TAK1 Covalently and Modulates Its Downstream Pathways in DoHH2 Cells. After we have established unequivocally the covalent nature of TAK1 inhibition by (5*Z*)-7-Oxozeaenol in cell free systems, we wanted to test whether a similar mode of action would take place inside the cells. B-NHL cell line DoHH2, which has constitutively activated p38 signaling driven by TAK1 activity, was treated with (5*Z*)-7-Oxozeaenol at several doses, and the impact on phosphorylation of p38 was monitored. Complete inhibition of p38 phosphorylation by (5*Z*)-7-Oxozeaenol was observed within 2 h of treatment at doses of 3 and 10 μM, and the effect was maintained with continuous exposure for at least 8 h (Figure 3A). After 16 h of continuous exposure to (5*Z*)-7-Oxozeaenol, we noticed a significant drop in cell viability resulting in poor yields of protein. Although the phosphorylation of p38 was still inhibited at 16 h, the level of total p38 also decreased compared to vehicle controls. To confirm that the effects of (5*Z*)-7-Oxozeaenol on TAK1 inhibition in cells was indeed irreversible, we conducted wash-out studies. DoHH2 cells were exposed to (5*Z*)-7-Oxozeaenol or an ATP-competitive reversible inhibitor of TAK1, AZ-TAK1 (for structure and characterization of this compound, see ref 20) for

dx.doi.org/10.1021/cb3005897 | *ACS Chem. Biol.* 2013, 8, 643−650

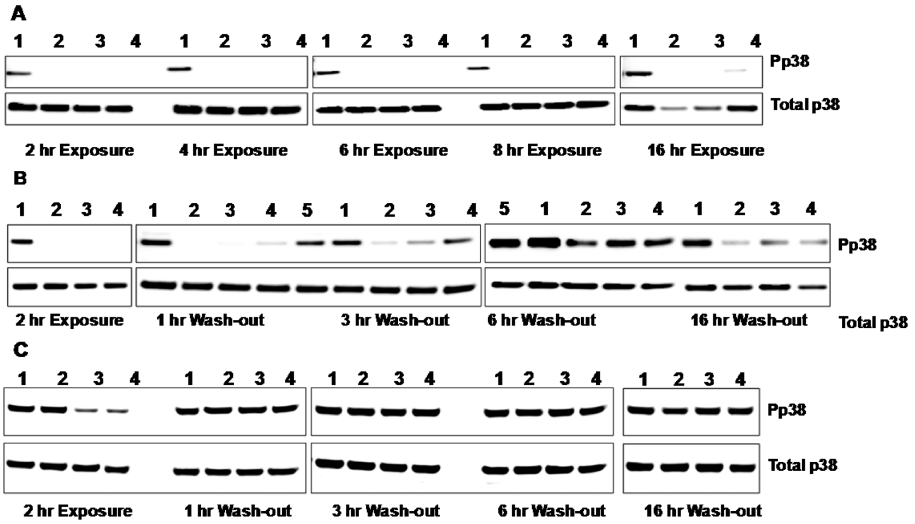

Figure 3. (5*Z*)-7-Oxozeaenol is an irreversible inhibitor of TAK1 in DoHH2 cells. Details of the experiment were described in Methods. (A) Kinetics of inhibition of TAK1 in DoHH2 cells after exposure to (5*Z*)-7-Oxozeaenol. Lane 1, DMSO vehicle; Lanes 2–4, (5*Z*)-7-Oxozeaenol at 30, 10, and 3 μM, respectively. (B) DoHH2 cells were treated with (5*Z*)-7-Oxozeaenol for 2 h followed by removal of drug and continued incubation of the cells for the noted wash-out periods. Lane 1, DMSO vehicle; Lanes 2–4, (5*Z*)-7-Oxozeaenol at 30, 10, and 3 μM, respectively; Lane 5, untreated cells (no vehicle). (C) Rapid recovery of p38 phosphorylation following treatment and removal of the reversible ATP-competitive inhibitor AZ-TAK1. Lane 1, untreated cells; Lane 2, DMSO vehicle; Lane 3, 1 μM AZ-TAK1; Lane 4, 0.3 μM AZ-TAK1.

2 h in order to achieve significant inhibition of p38 phosphorylation. After washing the cells with drug-free medium, aliquots were then taken at different time points to monitor how quickly TAK1 can regain its kinase activity by monitoring the recovery of phospho-p38 signal. Whereas AZ-TAK1 induced significant (~70%) inhibition of p38 phosphorylation within 2 h, the signal had returned to baseline within 1 h of compound removal (Figure 3C). By contrast, after removal of (5*Z*)-7-Oxozeaenol the phosphorylation of p38 was still inhibited by over 90% after 1 h and showed gradual recovery over the 6-h washout period in a dose-dependent manner. However by 6 h the signal had still not returned to baseline (Figure 3B). The assessment of recovery at later time points was hampered by the apparent toxicity of the compound at 16 h. Taken together, these data indicate that (5*Z*)-7-Oxozeaenol behaves in a different manner to a reversible ATP-competitive inhibitor and that the kinetics of TAK1 inhibition in cells is consistent with an irreversible mechanism.

Using (5*Z*)-7-Oxozeaenol as a tool compound, we demonstrated that TAK1 can be targeted irreversibly at both biochemical and cellular levels. Similar resorcyclic lactones have been shown to inhibit several kinases *via* covalent interaction.[15] Screening (5*Z*)-7-Oxozeaenol with a panel of 85 diverse kinases representing the kinome structural space showed that 11 of the 12 targeted kinases (>50% inhibition with 1 μM (5*Z*)-7-Oxozeaenol), including TAK1 kinase, contain a Cys residue before the DFG motif (Supplemental Table 4). There are roughly 46 kinases in the human kinome with a correctly positioned Cys residue in that region.[15] It can be envisioned that engineering an appropriately positioned Michael acceptor onto the scaffold of type I TAK1 kinase inhibitors should result in covalent inhibitors with improved or different selectivity. Traditionally discovery of kinase inhibitors has been focused on identification of classical type I reversible inhibitors mainly due to the concern for potential toxicity of covalent inhibitors from non-specific interactions in biological system. The application of Michael acceptors to irreversible inhibitor design well addressed such concerns. Michael acceptors including acrylamide and enone are relatively weaker electrophilic warheads that require a close proximity to targeted nucleophiles in order to form covalent bond,[3] thus significantly reducing non-specific modification of non-targeted proteins. Due to the relatively small size, Michael acceptors could be incorporated into existing optimized type I kinase inhibitors to further enhance selectivity without reducing the affinity of the parent compounds. The covalent crystal structure of TAK1 and (5*Z*)-7-Oxozeaenol will serve as a useful tool for designing the next generation of TAK1 irreversible inhibitors targeting Cys174, by incorporating an appropriately positioned Michael acceptor functional group onto reversible TAK1 inhibitor scaffolds, a strategy that has worked very effectively for developing irreversible kinase inhibitors.[21-23]

Sensitivity to TAK1 Inhibition by (5*Z*)-7-Oxoeaenol Is Associated with NRAS Mutation in Hematological Cancer Cell Lines. To further evaluate (5*Z*)-7-Oxozeaenol as a TAK1 specific inhibitor, we tested this compound in a cell line panel comprising 27 mixed hematological cancer lines to assess its anti-tumor activity *in vitro*. A distribution of sensitivity was observed with GI50s ranging from very sensitive (WSU-DLCL2, GI50 = 20 nM) to resistant (>32 μM GI50) as shown in Figure 4 and Supplemental Table 1. Interestingly, most of cell lines that are sensitive to (5*Z*)-7-Oxozeaenol harbor NRAS mutation (Fisher Exact test p-value =0.028). To better understand the molecular mechanism underlying (5*Z*)-7-Oxozeaenol sensitivity, we conducted gene expression profile analysis, and found that the expression of 312 probe-sets, representing 254 unique genes, were positively correlated to (5*Z*)-7-Oxozeaenol's pGI50 with Pearson's R > 0.45- (Supplemental Table 2). Subsequently, we applied IPA's core analysis for pathway enrichment to confirm that these are bona fide genes associated with TAK1 activity. Indeed, we found that these genes can be categorized into known TAK1 regulated pathways, including T cell signaling, macrophage biological processes, Rho signaling, and RANK signaling in osteoclasts and B cell receptor signaling (Supplemental Table 3). In addition, several transcription regulators that might be

dx.doi.org/10.1021/cb3005897 | *ACS Chem. Biol.* 2013, 8, 643–650

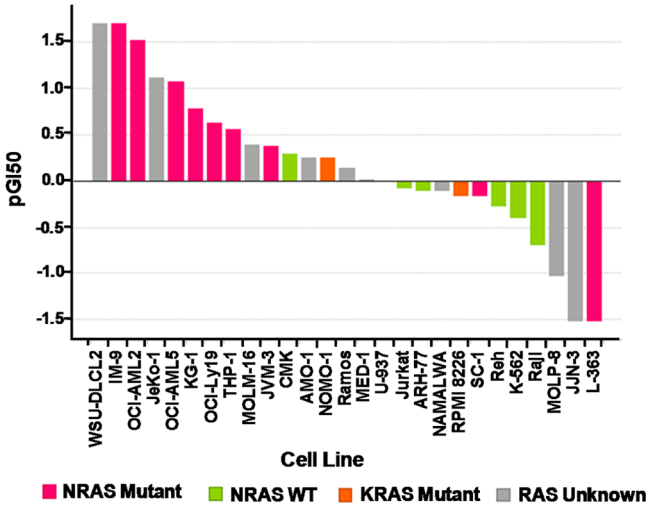

Figure 4. (5*Z*)-7-Oxozeaenol inhibition profile in 27 hematological cancer cell lines. GI50s were determined as described in Methods, and the values of GI50s in μM were $-\log_{10}$ transformed to pGI50 values. The NRAS status of each cell line was color coded.

responsible for regulating these genes were enriched, and those include HDAC1, PPARγ, CTNNB-TCF, NF-κB, and MYC. These transcription regulators have been associated with either Wnt or NF-κB pathways.[24,25]

Although (5*Z*)-7-Oxozeaenol showed significant inhibitory activity against several other kinases when it was tested with a kinase panel (Supplemental Table 4), this compound showed surprising specificity in inhibition of TAK1 pathway when it was tested with a cell panel, as shown by the strong enrichment of TAK1 regulated pathway genes in cell lines that are sensitive to (5*Z*)-7-Oxozeaenol inhibition (Figure 4, Supplemental Table 3). This observation supported the TAK1 on-target pharmacology of (5*Z*)-7-Oxozeaenol in hematological cancer cells. More interestingly, the top three transcription regulators identified in IPA analysis, HDAC1, PPARγ, and CTNNB-TCF, have been shown to be directly involved in, or cross-talk with, Wnt pathways. Specifically, Ye and co-workers demonstrated that in oligodendrocyte differentiation process, HDAC1 can crosstalk with canonical Wnt signaling pathway by competing with β-catenin for TCF7L2 interaction to regulate downstream genes.[24] Jansson and co-workers showed that in colon cancer cells, induction of Wnt/β-catenin pathway increased PPARγ gene and protein level, suggesting PPARγ to be a likely target of the Wnt pathway in cancer cells.[25] Nevertheless, the enrichment of a subset of Wnt related genes in cell lines sensitive to the TAK1 inhibition raised an interesting question on how TAK1 and Wnt pathways are linked in hematological cancer cells. This question is of relevance to another surprising observation we made in this study, that most of the sensitive cell lines carry NRAS mutations, the dominant RAS isoform alternations in liquid tumors as opposed to the KRAS mutation in solid tumors (Figure 4). NRAS and KRAS isoform mutations are mutually exclusive in cancers, and the two cell lines with KRAS mutation are also with medium sensitivity. Taken together, we propose that there is likely a previously unrecognized signaling network of NRAS-TAK1-Wnt, together with TAK1-NF-κB pathway, playing important roles in the growth and survival of certain hematological tumors. A similar signaling cascade has been demonstrated for solid cancer cells. Singh and co-workers showed that in a subset of KRAS-dependent, APC-deficient colon cancer cells, KRAS activated both Wnt and NF-κB pathways *via* the activation of TAK1.[26] More recently, Yu and co-workers demonstrated that non-canonical Wnt signaling is important for anchorage-independent growth of pancreatic tumor cells and their metastasis *in vivo*, and TAK1 inhibition can negate these effects.[27] Importantly, in both cases the inhibition of TAK1 activity was achieved by both small molecular inhibitor (5*Z*)-7-Oxozeaenol and genetic tools including TAK1 *si*RNA and *sh*RNA, corroborating that our finding in hematological cancer cells is *via* direct TAK1 inhibition. Together with our observation in hematological cancer cells, we suspect that TAK1 might be the convergent point for RAS signaling in both solid and liquid tumors. Further experimental work will be needed to confirm the linkage of NRAS, TAK1, and Wnt and its causative nature in hematological tumor settings.

METHODS

Materials. (5*Z*)-7-Oxozeaenol and other standard reagents were purchased from Sigma-Aldrich, unless otherwise mentioned. Compound AZ-TAK1 was synthesized by AstraZeneca scientists. Phospho-p38 (T180/Y182) specific antibody (cat. no. 9211) was purchased from Cell Signaling Technologies. The baculovirus expression vector pFastBac was purchased from Life Technologies. The TAK1-TAB1 fusion protein was obtained following previous examples.[12,13] DoHH2 cells were purchased from ATCC. Cells were cultured in RPMI 1640 medium (Life Technologies) supplemented with 10% FBS (Hyclone) and 2 nM L-glutamine and maintained at 37 °C in 5% CO_2.

TAK1-TAB1 Activity Assay. The TAK1-TAB1 PK/LDH coupled assay was conducted to detect ADP formation at RT on 384-well UV plates (Corning), and readout was the decrease of absorbance at 340 nm due to NADH consumption. The standard reactions, except where indicated, were carried out in a final volume of 40 μL, in pH 7.4 HEPES buffer. In a typical experiment, the reaction mixture including PK/LDH coupling components, ATP, and inhibitor if required was pre-incubated at RT for 5 min before TAK1-TAB1 protein was added to initiate the reactions. Reactions were allowed to proceed until the progress curves became linear, indicating that the steady state was attained. ATPase activity of TAK1-TAB1, *i.e.*, the ATP hydrolytic activity, was also assessed using Malachite Green colorimetric assay. This assay detects inorganic phosphate, the other product generated from TAK1-TAB1 ATPase reaction. Reactions were set up in transparent 384-well plates (Corning) using the same buffer as the PK/LDH coupled assay and quenched by adding a detection mixture made of Malachite Green dye. The plates were read after 6 min incubation at RT at 650 nm on a Molecular Devices plate reader.

Data analysis. For calculation of the rate of TAK1-TAB1 inactivation by (5*Z*)-7-Oxozeaenol, reaction progress curves from PK/LDH coupled assay were fit to the integrated rate equation (eq 1) for irreversible inhibition [28] by nonlinear regression analysis using GraFit 5 (Erithacus Software).

$$A_t = A_0 - v_s t - (v_i - v_s)(1 - e^{-k_{obs}t})/k_{obs} \quad (1)$$

In eq 1, A_t and A_0 are the absorbance at time t and time 0, respectively, k_{obs} is the pseudo-first-order rate constant for reactions to reach the steady state, and v_i and v_s correspond to the initial and final slopes of the progress curve. Values for v_i, v_s, and k_{obs} were obtained at each inhibitor concentration and further analyzed following a two-step inhibition mechanism described by Figure 1D, where the initial rapid binding of the inhibitor to enzyme is followed by a second slower step that results in the final enzyme−inhibitor complex. To obtain the equilibrium and kinetic constants eq 2 was used, where k_{inact} is the rate constant for inactivation, K_I is the apparent inhibition constant, S is the ATP concentration, and K_M is the Michaelis−Menten constant for ATP (Table 1).

$$k_{obs} = k_{inact} I/(K_I(1 + S/K_M) + I) \quad (2)$$

dx.doi.org/10.1021/cb3005897 | *ACS Chem. Biol.* 2013, 8, 643−650

Mass Spectrometry. Covalent modification of TAK1-TAB1 by (5*Z*)-7-Oxozeaenol was studied by mass spectrometry. Briefly, reactions of 1 μM TAK1-TAB1 with 1 μM of inhibitor were made in a final volume of 400 μL, in HEPES buffer. Aliquots were withdrawn from the reactions at different time points and snap-frozen in liquid N_2. Control samples contained DMSO instead of inhibitor. Intact protein samples were analyzed by positive ion ESI-MS on a QSTAR Pulsar *i* mass spectrometer (Applied Biosystems) equipped with a Turbo Ion Spray source. Protein mass spectra were de-convoluted using Analyst QS software (version 1.1). Relative peak intensity of modified and unmodified proteins were recorded and fitted to a first-order exponential equation to estimate the observed rate of protein modification (Table 1).

X-ray Crystallography. De-phosphorylated TAK1-TAB1 was crystallized as described with minor modification.[13] Crystals grew by vapor diffusion at RT. Optimal conditions were obtained in 3 μL hanging drops containing equal parts of protein and reservoir solution of 0.55−0.75 M sodium citrate, 0.2 M NaCl, 0.1 M Tris pH 7.0, and 5 mM adenosine. Crystals appeared overnight and grew over several days. Crystals with adenosine were then back-soaked in solutions with excess inhibitor. Diffraction data were obtained in house to 2.2 Å resolution from an FRE+ generator outfitted with a CCD detector. Data were integrated and scaled using d*Trek software [29] (Table 2). The structure was determined by molecular replacement using AMoRe28 and refined using Refmac [30] with rebuilding in Coot.[31] Final refinement statistics converged with R_{work} = 0.221 and R_{free} = 0.245. The final density surrounding the inhibitor was excellent.

Cell Wash-out Assay. Inhibition of p38 phosphorylation was evaluated with DoHH2 cells by Western blot. Specifically, cells were treated with either inhibitor or vehicle (DMSO) control, and an aliquot of cells was removed for each time point and washed with 1x cold PBS. Subsequently whole cell lysates were prepared and evaluated by Western blot. To evaluate the duration of inhibition effect, DoHH2 cells were treated with either inhibitor or DMSO for 2 h, and the media were removed after centrifugation. Subsequently the cells were washed three times with fresh medium and re-suspended in fresh medium. Aliquots of cells were taken at several time points after washout and subjected to Western blot to evaluate total p38 and phospho-p38 levels. Western blot analysis was conducted following standard procedure. Primary antibodies were detected using goat anti-rabbit IgG HRP-linked secondary antibody diluted 1:10000 and incubated at RT for 1 h. The blots were developed using Signal West Dura Extended Duration Substrate (ThermoFisher Scientific). All bands were detected and quantified using the Fuji Imager System (Life Science USA).

Anti-proliferation Cell Assay. Anti-proliferative effect of (5*Z*)-7-Oxozeaenol was assessed on an AstraZeneca internal cancer cell panel comprising 27 hematological cancer cell lines of different types using alamar blue method. All cell lines were cultured and plated in RPMI-1640 media with 10% FBS and 2 mM L-glutamine in 96-well plates. Plates developed on the day of compound addition were referred to as Day 0. Dosed plates were cultured 3 days under normal conditions. After 3 days of culture, dosed plates were developed using alamar blue. For each inhibitor concentration, percentage net growth was calculated by (Day 3 dosed well − Average Day 0)/(Average Day 3 DMSO control − Average Day 0). The GI50 of each inhibitor was computed using the percentage net growth as defined by NCI.

Bio-informatic Analysis. Cell line gene expression was measured using Affymetrix HG U133 Plus2.0 GeneChip arrays following the standard protocol suggested by the manufacturer. Gene expression level was quantified using MAS 5.0 with scaling set to 100. The signal values were $\log_2$ transformed. Probe sets whose mean values in the panel were less than 4.5 were filtered out. GI50 values in μM of (5*Z*)-7-Oxozeaenol were $\log_{10}$ transformed and correlated with individual probe-set's expression values using Pearson's R. Probe-sets with Pearson's *R* greater than 0.45 were selected. Pathway enrichment analysis was performed using Ingenuity's IPA with default settings. For mutation analysis, Fisher's exact test was used to calculate the *p*-value.

■ ASSOCIATED CONTENT

Supporting Information

This material is available free of charge *via* the Internet at http://pubs.acs.org.

Accession Codes

PDB code 4GS6.

■ AUTHOR INFORMATION

Corresponding Author

*E-mail: jiaquan.wu@astrazeneca.com; raymond.chen@astrazeneca.com.

Notes

The authors declare no competing financial interest.

■ ACKNOWLEDGMENTS

We thank F. Gharahdaghi for assisting with MS analysis, X. Zhu and S. Livchak for protein expression and purification, T. Cheung for assistance with kinase profiling, and A. Ferguson for assistance with refinement.

■ REFERENCES

(1) Davis, M. I., Hunt, J. P., Herrgard, S., Ciceri, P., Wodicka, L. M., Pallares, G., Hocker, M., Treiber, D. K., and Zarrinkar, P. P. (2011) Comprehensive analysis of kinase inhibitor selectivity. *Nat. Biotechnol. 29*, 1046−1051.

(2) Copeland, R. A., Pompliano, D. L., and Meek, T. D. (2006) Drug-target residence time and its implications for lead optimization. *Nat. Rev. Drug Discovery 5*, 730−739.

(3) Singh, J., Petter, R. C., Baillie, T. A., and Whitty, A. (2011) The resurgence of covalent drugs. *Nat. Rev. 10*, 307−317.

(4) Barf, T., and Kaptein, A. (2012) Irreversible protein kinase inhibitors: balancing the benefits and risks. *J. Med. Chem. 26*, 6243−6262.

(5) Takaesu, G., Surabhi, R. M., Park, K. J., Ninomiya-Tsuji, J., Matsumoto, K., and Gaynor, R. B. (2003) TAK1 is critical for IkappaB kinase-mediated activation of the NF-kappaB pathway. *J. Mol. Biol. 326*, 105−115.

(6) Ninomiya-Tsuji, J., Kishimoto, K., Hiyama, A., Inoue, J., Cao, Z., and Matsumoto, K. (1999) The kinase TAK1 can activate the NIK-I kappaB as well as the MAP kinase cascade in the IL-1 signaling pathway. *Nature 398*, 252−256.

(7) Lee, J., Mira-Arbibe, L., and Ulevitch, R. J. (2000) TAK1 regulates multiple protein kinase cascades activated by bacterial lipopolysaccharide. *J. Leukocyte Biol. 68*, 909−915.

(8) Sun, L., Deng, L., Ea, C. K., Xia, Z. P., and Chen, Z. J. (2004) The TRAF6 ubiquitin ligase and TAK1 kinase mediate IKK activation by BCL10 and MALT1 in T lymphocytes. *Mol. Cell 14*, 289−301.

(9) Sato, S., Sanjo, H., Takeda, K., Ninomiya-Tsuji, J., Yamamoto, M., Kawai, T., Matsumoto, K., Takeuchi, O., and Akira, S. (2005) Essential function for the kinase TAK1 in innate and adaptive immune responses. *Nat. Immunol. 11*, 1087−1095.

(10) Shinohara, H., Yasuda, T., Aiba, Y., Sanjo, H., Hamadate, M., Watarai, H., Sakurai, H., and Kurosaki, T. (2005) PKC beta regulates BCR-mediated IKK activation by facilitating the interaction between TAK1 and CARMA1. *J. Exp. Med. 202*, 1423−1431.

(11) Yamaguchi, K., Shirakabe, K., Shibuya, H., Irie, K., Oishi, I., Ueno, N., Taniguchi, T., Nishida, E., and Matsumoto, K. (1995) Identification of a member of the MAPKKK family as a potential mediator of TGF-beta signal transduction. *Science 270*, 2008−2011.

(12) Sakurai, H., Nishi, A., Sato, N., Mizukami, J., Miyoshi, H., and Sugita, T. (2002) TAK1-TAB1 fusion protein: a novel constitutively active mitogen-activated protein kinase kinase kinase that stimulates AP-1 and NF-kappaB signaling pathways. *Biochem. Biophys. Res. Commun. 297*, 1277−1281.

(13) Brown, K., Vial, S. C., Dedi, N., Long, J. M., Dunster, N. J., and Cheetham, G. M. (2005) Structural basis for the interaction of TAK1 kinase with its activating protein TAB1. *J. Mol. Biol. 354*, 1013−1020.
(14) Ohori, M., Kinoshita, T., Yoshimura, S., Warizaya, M., Nakajima, H., and Miyake, H. (2007) Role of a cysteine residue in the active site of ERK and the MAPKK family. *Biochem. Biophys. Res. Commun. 353*, 633−637.
(15) Schirmer, A., Kennedy, J., Murli, S., Reid, R., and Santi, D. V. (2006) Targeted covalent inactivation of protein kinases by resorcylic acid lactone polyketides. *Proc. Natl. Acad. Sci. U.S.A. 103*, 4234−4239.
(16) Ninomiya-Tsuji, J., Kajino, T., Ono, K., Ohtomo, T., Matsumoto, M., Shiina, M., Mihara, M., Tsuchiya, M., and Matsumoto, K. (2003) A resorcylic acid lactone, 5Z-7-oxozeaenol, prevents inflammation by inhibiting the catalytic activity of TAK1MAPK kinase kinase. *J. Biol. Chem. 278*, 18485−18490.
(17) Rominger, C. M., Schaber, M. D., Yang, J., Gontarek, R. R., Weaver, K. L., Broderick, T., Carter, L., Copeland, R. A., and May, E. W. (2007) An intrinsic ATPase activity of phospho-MEK-1 uncoupled from downstream ERK phosphorylation. *Arch. Biochem. Biophys. 464*, 130−137.
(18) Fox, T., Fitzgibbon, M. J., Fleming, M. A., Hsiao, H. M., Brummel, C. L., and Su, M. S. (1999) Kinetic mechanism and ATP-binding site reactivity of p38g MAP kinase. *FEBS Lett. 461*, 323−328.
(19) Rastelli, G., Rosenfeld, R., Reid, R., and Santi, D. V. (2008) Molecular modeling and crystal structure of ERK2-hypothemycin complexes. *J. Struct. Biol. 164*, 18−23.
(20) Buglio, D., Palakurthi, S., Byth, K., Vega, F., Toader, D., Saeh, J., Neelapu, S. S., and Younes, A. (2012) Essential role of TAK1 in regulating mantle cell lymphoma survival. *Blood 120*, 347−355.
(21) Wissner, A., and Mansour, T. S. (2008) The development of HKI-272 and related compounds for the treatment of cancer. *Arch. Pharm. (Weinheim) 341*, 465−477.
(22) Yap, T. A., Vidal, L., Adam, J., Stephens, P., Spicer, J., Shaw, H., Ang, J., Temple, G., Bell, S., Shahidi, M., Uttenreuther-Fischer, M., Stopfer, P., Futreal, A., Calvert, H., de Bono, J. S., and Plummer, R.. (2010) Phase I trial of the irreversible EGFR and HER2 kinase inhibitor BIBW 2992 in patients with advanced solid tumors. *J. Clin. Oncol. 28*, 3965−3972.
(23) Pan, Z., Scheerens, H., Li, S. J., Schultz, B. E., Sprengeler, P. A., Burrill, L. C., Mendonca, R. V., Sweeney, M. D., Scott, K. C., Grothaus, P. G., Jeffery, D. A., Spoerke, J. M., Honigberg, L. A., Young, P. R., Dalrymple, S. A., and Palmer, J. T. (2007) Discovery of selective irreversible inhibitors for Bruton's tyrosine kinase. *ChemMedChem. 2*, 58−61.
(24) Ye, F., Chen, Y., Hoang, T., Montgomery, R. L., Zhao, X. H., Bu, H., Hu, T., Taketo, M. M., van Es, J. H., Clevers, H., Hsieh, J., Bassel-Duby, R., Olson, E. N., and Lu, Q. R. (2009) HDAC1 and HDAC2 regulate oligodendrocyte differentiation by disrupting the beta-catenin-TCF interaction. *Nat. Neurosci. 12*, 829−838.
(25) Jansson, E. A., Are, A., Greicius, G., Kuo, I. C., Kelly, D., Arulampalam, V., and Pettersson, S. (2005) The Wnt/β-catenin signaling pathway targets PPARγ activity in colon cancer cells. *Proc. Natl. Acad. Sci. U.S.A. 102*, 1460−1465.
(26) Singh, A., Sweeney, M. F., Yu, M., Burger, A., Greninger, P., Benes, C., Haber, D. A., and Settleman, J. (2012) TAK1 inhibition promotes apoptosis in KRAS-dependent colon cancers. *Cell. 148*, 639−650.
(27) Yu, M., Ting, D. T., Stott, S. L., Wittner, B. S., Ozsolak, F., Paul, S., Ciciliano, J. C., Smas, M. E., Winokur, D., Gilman, A. J., Ulman, M. J., Xega, K., Contino, G., Alagesan, B., Brannigan, B. W., Milos, P. M., Ryan, D. P., Sequist, L. V., Bardeesy, N., Ramaswamy, S., Toner, M., Maheswaran, S., and Haber, D. A. (2012) RNA sequencing of pancreatic circulating tumor cells implicates WNT signaling in metastasis. *Nature 487*, 510−513.
(28) Morrison, J. F., and Walsh, C. T. (1988) Adv Enzymol Relat Areas. *Mol. Biol. 61*, 201−301.
(29) Pflugrath, J. W. (1999) The finer things in X-ray diffraction data collection. *Acta Crystallogr., Sect. D 55*, 1718−1725.
(30) Bailey, S. (1994) The CCP4 suite - programs for protein crystallography. *Acta Crystallogr., Sect. D 50*, 760−763.
(31) Emsley, P., Lohkamp, B., Scott, W. G., and Cowtan, K. (2010) Features and development of Coot. *Acta Crystallogr., Sect. D 66*, 486−501.